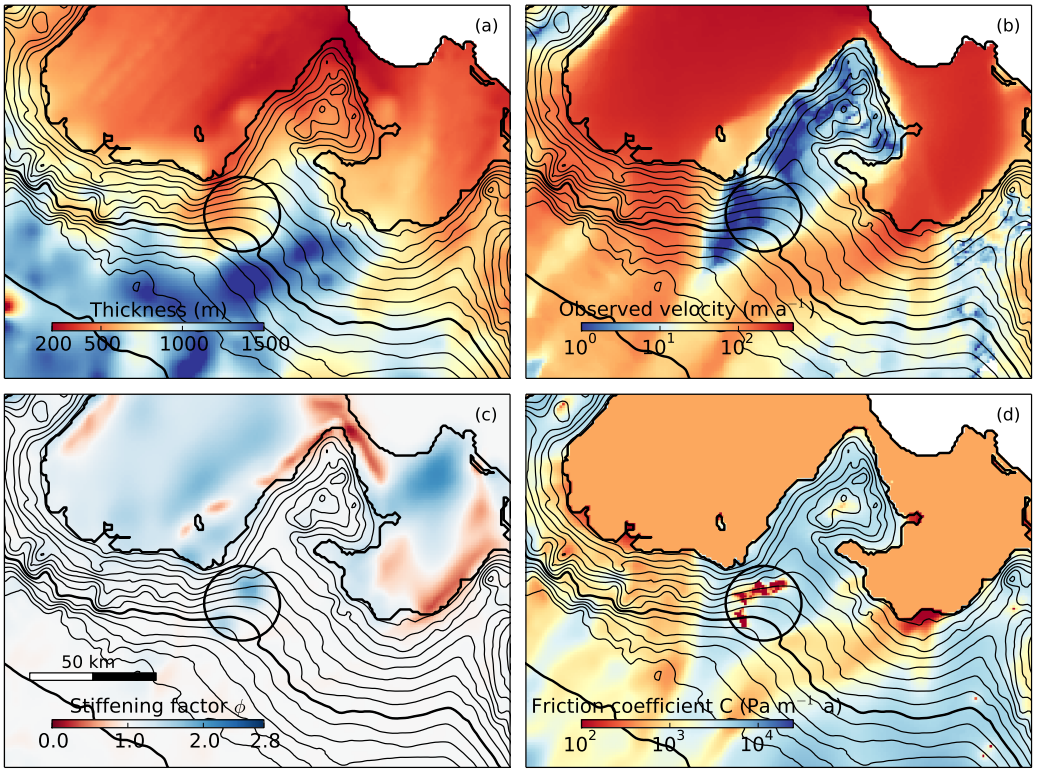

Figure S1. Results of the data assimilation for linear sliding focussing on the TB/HB promontory where high velocity mismatch (shown by a circle) occurs due to poor consistency between the observations of high surface gradients and low surface velocities (Figure 4). (a) Thickness, (b) observed velocities, (c) stiffening factor and (d) friction coefficient. Contours show ice surface elevation every 50 m in the range 100-800 m.

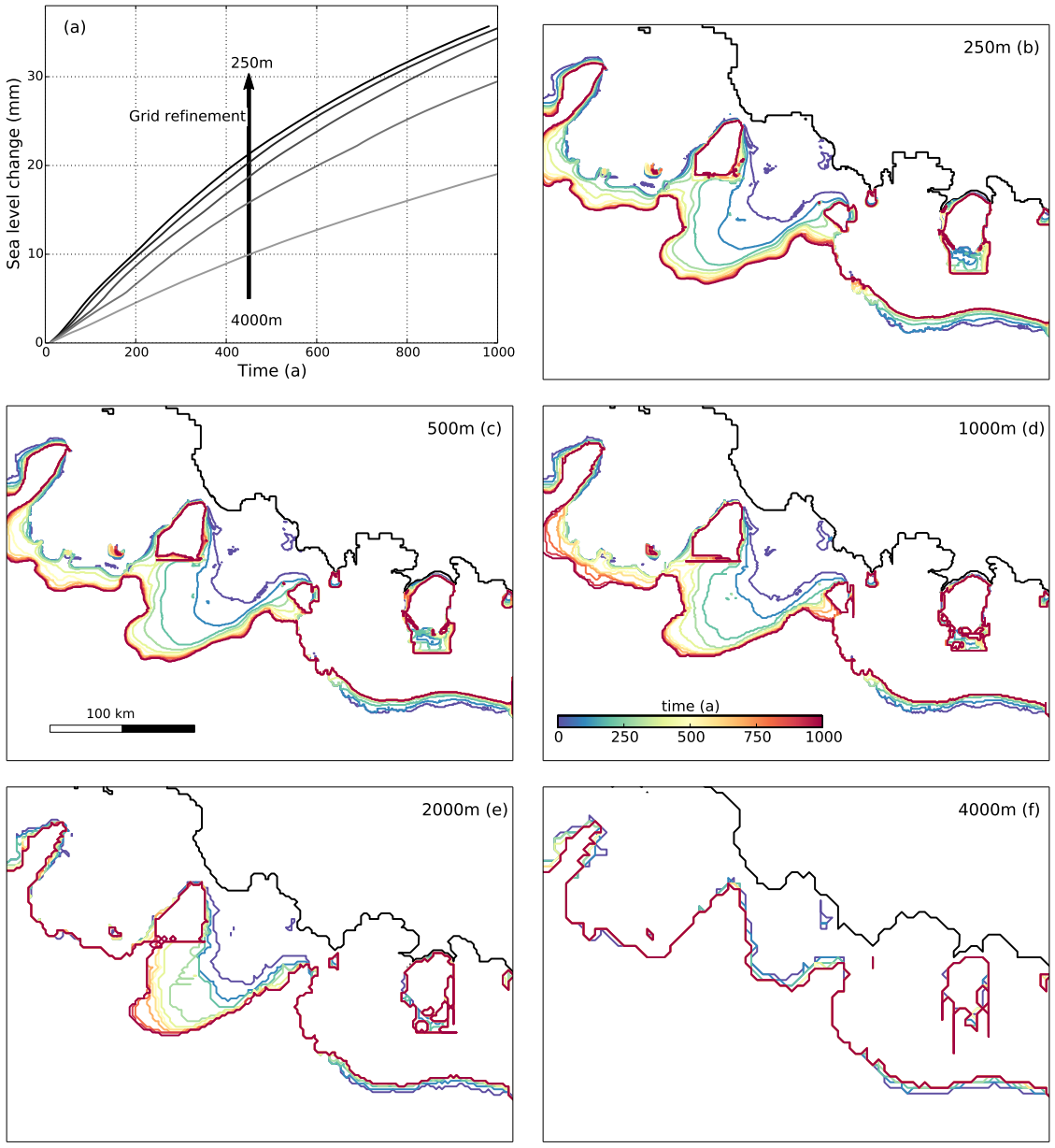

Figure S2. sensitivity to grid resolution between 250 m and 4000 m at the grounding line, performed for the $B_e/S/L/M_{b1}/A_m$ experiment. (a) Cumulative sea level changes. The 4000 m resolution simulation results in the lowest changes while the 250 m resolution results in the highest changes. The differences between 250 m and 500 m are not significant. The 500 m resolution was therefore chosen to run all the simulations discussed in the main paper. (b) to (f) Grounding-lines shown every 100 years (colorscale shown in (d)) for the resolution indicated at the top right of each panel.

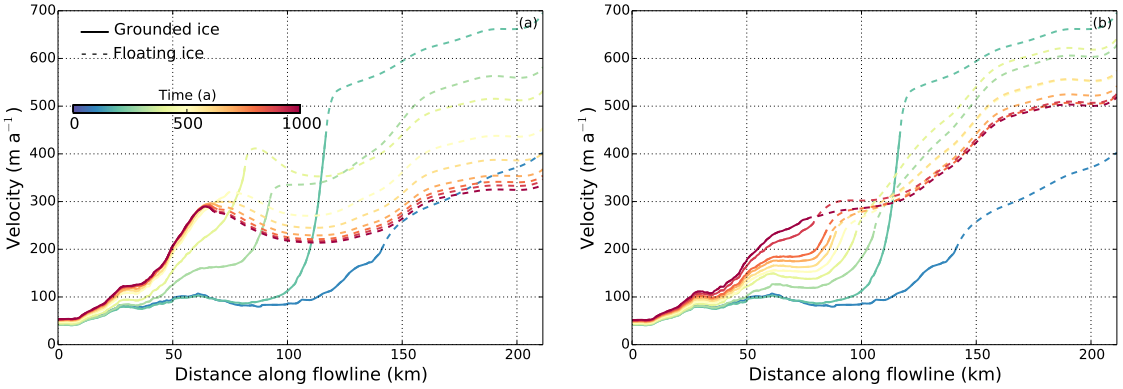

Figure S3. Ice velocity profiles shown every 100 years for the (a) $B_e/S/L/M_{b1}/A_m$ experiment along the flowline shown in Figure 6(a), and (b) for the same experiment in which the sub ice-shelf melting is switched off beneath the Hansenbreen ice shelf when the grounding line retreats over the upsloping part of the bed. The sub ice-shelf melting for other parts of the computational domain are not altered. The grounding line position is marked by the limit between solid and dashed parts of profiles.

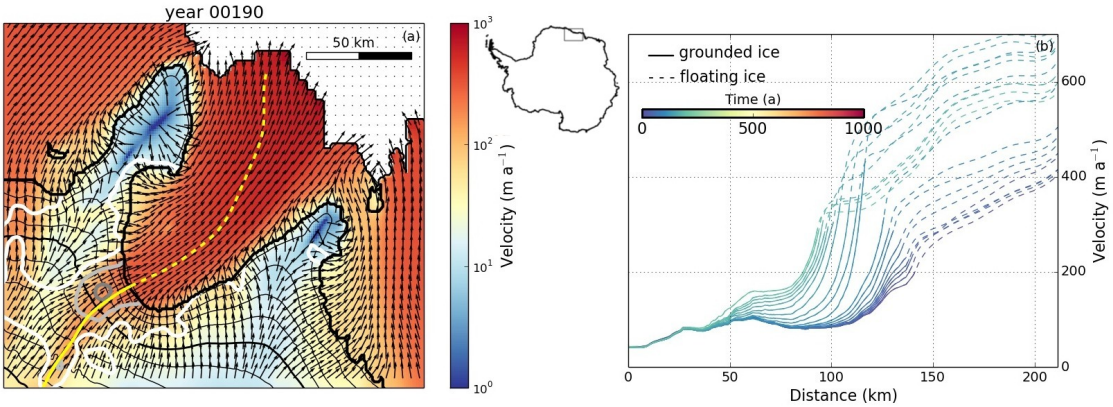

Movie S1. Ice-sheet changes in Hansenbreen for the next millennium simulated by the $B_e/S/L/M_1/A_m$ experiment, shown every decade. (a) Migration of the grounding line: flow-field from Berger et al. (2016) in the background, with ice-flow direction indicated by the arrows, the thick black lines show the grounding line and the calving front, ice-surface elevation contours every 100 m and a flowline is shown in yellow. (b) Ice velocity profiles along the (a) flowline: the solid and dashed black lines indicates grounded and floating ice (shown here for the year 190 after relaxation).

Table S1. Observed and initially modelled sub-ice shelf melt rates by drainage basins in Gt a^{-1}, from West to East within the computational domain (Figure 1). Our initial melt rates are comparable to what is given in Rignot et al. (2013) and to a Personal Communication (PC) from M. Depoorter (using the same technique as in Depoorter et al. (2013)). The exact numbers could not be reproduced for the medium melt-rates experiments since the sub-ice shelf melt rates are constrained by unique values over the computational domain. LIS: Lazarev ice shelf; UG: Unnamed Glacier; TB: Tussebreen; HB: Hansenbreen; RBIS: Roi Baudouin ice shelf.

Glacier		LIS	UG	TB	HB	RBIS	total
Observations	Depoorter et al. (2013) + PC	1.8	0.5	3.6	3.7	20.2	29.8
	Rignot et al. (2013)	6.3	7.5 (UG+TB+HB)			14.1	27.9
Simulations	Low rates	0.65±0.05	2.5±0.5	2.75±0.25	1.5±0.5	7±1	15±0.5
	Medium rates	1.4±0.2	4.5±0.4	4.9±0.1	2.5±0.5	14±2	28±2
	High rates	2.2±0.3	6.9±0.4	7.1±0.15	4.5±1.5	22±3	42±2

References

Berger, S., Favier, L., Drews, R., Derwael, J.-J., and Pattyn, F.: The control of an uncharted pinning point on the flow of an Antarctic ice shelf, Journal of Glaciology, 62, 37–45, doi:10.1017/jog.2016.7, 2016.

Depoorter, M. a., Bamber, J. L., Griggs, J. a., Lenaerts, J. T. M., Ligtenberg, S. R. M., van den Broeke, M. R., and Moholdt, G.: Calving fluxes and basal melt rates of Antarctic ice shelves., Nature, 502, 89–92, doi:10.1038/nature12567, URL http://www.ncbi.nlm.nih.gov/pubmed/24037377, 2013.

Rignot, E., Jacobs, S., Mouginot, J., and Scheuchl, B.: Ice-Shelf Melting Around Antarctica, Science, 341, 266–270, doi:10.1126/science.1235798, URL http://www.sciencemag.org/cgi/doi/10.1126/science.1235798, 2013.